Instantons, diquarks, and nonleptonic weak decays of hyperons

M. Cristoforetti,[1] P. Faccioli,[2,3] E.V. Shuryak,[4] and M. Traini[3,5]
[1]*Dipartimento di Fisica, Università degli Studi di Milano, Via Celoria 16, I-20133 Milano, Italy*
[2]*ECT*, 286 Strada delle Tabarelle, Villazzano (Trento), I-38050 Italy*
[3]*INFN, Gruppo Collegato di Trento, Povo (Trento), Italy*
[4]*Department of Physics and Astronomy, SUNY at Stony Brook, Stony Brook, New York 11794, USA*
[5]*Dipartimento di Fisica, Università degli Studi di Trento, Via Sommarive 14, I-38050 Povo, Italy*
(Received 3 March 2004; published 16 September 2004)

This work is devoted to the study of the nonperturbative contributions in nonleptonic hyperon decays. We show that the instanton-induced 't Hooft interaction can naturally explain the $\Delta I = 1/2$ rule, by generating quark-diquark clustering inside octet baryons. We compute P-wave and S-wave amplitudes in the instanton liquid model, and find good agreement with experiment. We propose a model-independent procedure to test on the lattice if the leading quark-quark attraction in the 0^+ antitriplet channel responsible for diquark structures in hadrons is originated by the interaction generated by quasiclassical fields or if it is predominantly due to other perturbative and/or confining forces.

DOI: 10.1103/PhysRevD.70.054016 PACS numbers: 12.38.–t, 13.30.–a

I. INTRODUCTION

Weak decays of hadrons encode important information about the meson and baryon structure and about the QCD interactions in the perturbative and nonperturbative regimes. The natural scale of weak processes—set by W boson mass—is much larger than all other scales involved in the hadron internal dynamics. This implies that weak interactions are effectively local and therefore can resolve short-distance structures inside hadrons. Moreover, their explicit dependence on quark flavor and chirality can be exploited to probe the Dirac and flavor structure of the nonperturbative QCD interaction.

Among the large variety of weak hadronic processes, a prominent role is played by the nonleptonic decays of kaons and hyperons, which are characterized by the famous $\Delta I = 1/2$ rule [1]. With this name, one refers to the empirical observation that amplitudes in which the total isospin is changed by $1/2$ units are roughly 20 times larger than the corresponding amplitudes in which the isospin is changed by $3/2$ units.

Despite nearly 40 years of efforts, the microscopic dynamical mechanism responsible for such a striking phenomenon is still elusive. Neither electroweak nor *perturbative* QCD interactions can account for the dramatic relative enhancement of the $\Delta I = 1/2$ decay channels. Its origin must therefore reside in the nonperturbative sector of QCD.

Important insight on the role of nonperturbative dynamics in nonleptonic hyperon decays has come from the observation that in the pole model (see below) the suppression of the decays in the $\Delta I = 3/2$ channel can be explained if the quarks participating to the weak decay are in an antisymmetric color combination (Pati-Woo theorem, [2]). Unfortunately, in a simple constituent quark-model picture it is not easy to obtain satisfactory *quantitative* predictions for both the P-wave and the S-wave amplitudes. One usually needs to make additional model assumptions on the pole-model part of the amplitude, and this somewhat spoils the simplicity of the approach. For example, in order to reproduce the data on S-wave amplitudes, one needs to include $1/2^-$ intermediate states [3].

From these considerations it follows that further investigations are still needed in order to understand the nonperturbative QCD dynamics underlying nonleptonic weak decays. In particular, it would be desirable to set up a field-theoretic calculation which accounts explicitly for the current quark and gluon degrees of freedom. In this work, we explore the possibility that the phenomenology of hyperon decays can be understood in the instanton liquid model (ILM). Such an approach is derived directly from the QCD Lagrangian, by selecting a specific set of gauge configurations which are assumed to dominate the path integral.

Instantons are topological gauge configurations which dominate the QCD path integral in the semiclassical limit. They generate an effective quark-quark interaction ('t Hooft vertex) which breaks spontaneously chiral symmetry and solves the U(1) problem [4]. Evidence for instanton-induced dynamics has been accumulated over the years from a variety of phenomenological studies [5] as well as from lattice simulations [6–9]. In general, these nonperturbative vacuum fields play an important role in the chiral dynamics of light quarks [10], but it is generally believed that they do not provide an areal law for the Wilson loop.

The ILM assumes that the QCD vacuum is saturated by an ensemble of instantons and anti-instantons. The two phenomenological parameters of the model are the instanton average size ($\bar{\rho} \simeq 1/3$ fm) and average density ($\bar{n} \simeq 1$ fm^{-4}). These values were first extracted 20 years

ago from the global properties of the QCD vacuum (quark and gluon condensates) [11].

In the ILM, quarks are bound by the 't Hooft interaction. Even in the absence of confinement, the structure of the lowest-lying part of the light meson and baryon spectra is very well reproduced [12–14]. In particular, in this model the lightest octet of pseudoscalar and vector mesons as well as the lightest octet and decuplet of baryons have very realistic masses. Moreover, the short-range forces generated by instantons allow one to reproduce the available experimental data on the pion and nucleon form factors and more generally explain the delay of the onset of the asymptotic perturbative regime, in hard exclusive reactions [15,16].

Besides providing a successful overall description of the light hadron phenomenology, instantons have a specific property which makes them natural candidates for the solution of the $\Delta I = 1/2$ problem. In fact, Stech, Neubert, and Xu pointed out that the body of data on nonleptonic kaon and hyperon decays can be simultaneously reproduced, if one assumes that the nonperturbative quark-quark interaction in the color antitriplet channel is sufficiently attractive to form colored quasibound structures (diquarks) inside hadrons [17]. Instantons provide a microscopic mechanism which generates such a strong attraction binding scalar diquarks [13] and leading to quark-diquark clustering inside the octet baryons.

In the past there have been few attempts to understand the $\Delta I = 1/2$ rule with instantons [18,19]. In [18], Kochelev and Vento (KV) computed the instanton contribution to nonleptonic kaon decays. On a qualitative level, they found that the inclusion of the instanton effects indeed produces a strong enhancement of the $\Delta I = 1/2$ decay channel. On a quantitative level, such an enhancement was found to be still insufficient to reproduce the experimental data. However, it should be mentioned that nonleptonic kaon decays in the $\Delta I = 1/2$ channel receive a large contribution also from final-state interactions, which have not been included in the KV analysis. Moreover, it is now clear that the KV calculation is undershooting the instanton contribution.[1]

In [19] the instanton-induced corrections to the effective Hamiltonian for $\Delta S = 1$ transitions were analyzed in the framework of the operator product expansion (OPE). They found that such "hard" instanton effects are rather small. This result is not surprising: The instanton field cannot transfer momenta much larger than its inverse size $1/\bar{\rho} \sim 0.6$ GeV, so instanton effects above such a scale are exponentially suppressed. For this reason, in order to draw conclusions about the role played by the 't Hooft interaction in weak decays, one necessarily needs to include their contribution to the "soft" hadronic matrix elements. In view of these arguments, in the present analysis we shall neglect all instanton corrections above the hadronic scale set by the inverse instanton size $\mu = 1/\bar{\rho}$ and compute their contributions to low-energy matrix elements.

The paper is organized as follows. In Sec. II we analyze the structure of the effective Hamiltonian for $\Delta S = 1$ transitions and explain in detail why instantons are expected to produce strong enhancement of the matrix elements associated to $\Delta I = 1/2$ transitions. In Sec. III we review the framework which allows one to connect parity-conserving and parity-violating decay amplitudes to low-energy matrix elements of local operators. The calculation of the decay amplitudes in the ILM is presented in Sec. IV. In Sec. V we discuss our results and address the question of how to check our model assumption of instanton domination for the light hadron dynamics. We shall propose a systematic procedure to determine on the lattice if the strong quark-quark attractive interaction in the antitriplet 0^+ channel (which drives the $\Delta I = 1/2$ rule) is predominantly due to quasiclassical gauge configurations or is instead generated by other nonquasiclassical fields, associated to quark confinement. All results and conclusions are summarized in Sec. VI.

II. $\Delta S = 1$ EFFECTIVE HAMILTONIAN AND THE ORIGIN OF THE $\Delta I = \frac{1}{2}$ RULE

To lowest order in the Weinberg-Glashow-Salam Lagrangian, nonleptonic weak decays are driven by a single W-boson exchange. However, such processes receive also QCD and QED corrections. These contributions are usually included in the framework of OPE, in which one separates short-distance hard dynamics from large-distance soft dynamics. The former interactions can be treated perturbatively and give rise to the well-known effective weak Hamiltonian, which for $\Delta S = 1$ transitions reads [21]

$$H_{\rm eff}^{\Delta S=1} = \frac{G_F}{\sqrt{2}} V_{ud} V_{us} \left\{ \sum_{i=\pm,3,5,6} c_i(\mu) Q_i + \text{H.c.} \right\}. \quad (1)$$

G_F is the Fermi constant, V_{ud} and V_{us} are quark mixing matrix elements, Q_i are local four-quark operators, and $c_i(\mu)$ are the corresponding Wilson coefficients (μ is the hadronic scale). The local operators Q_i can be written as

[1]The KV calculation was performed in the single-instanton approximation. In such an approach, one treats explicitly the degrees of freedom of the closest instanton and introduces an additional parameter m^*, which effectively encodes contributions from all other instantons. In their calculation, the authors adopted the phenomenological estimate for m^* which was available at the time, $m^* \simeq 260$ MeV. Later, the same parameter was rigorously defined, and determined from numerical simulations in the ILM [20]. It was found to be considerably smaller ($m^* \simeq 80$ MeV).

$$
\begin{aligned}
Q_{\pm} &= \frac{1}{2}[(\bar{u}s)_{V-A}(\bar{d}u)_{V-A} \pm (\bar{d}s)_{V-A}(\bar{u}u)_{V-A}], \\
Q_{3,5} &= (\bar{d}s)_{V-A} \sum_{q=u,d,s} (\bar{q}q)_{V\mp A}, \\
Q_6 &= -2 \sum_{q=u,d,s} (\bar{q}s)_{S+P}(\bar{d}q)_{S-P},
\end{aligned} \tag{2}
$$

where we have adopted the notations $(\bar{q}q)_{V\pm A} = \bar{q}\gamma_\mu(1 \pm \gamma_5)q$ and $(\bar{q}q)_{S\pm P} = \bar{q}(1 \pm \gamma_5)q$.

For a typical hadronic scale, $\mu \simeq 1$ GeV, the numerical values of the Wilson coefficients are $c_+ = 0.72$, $c_- = 1.97$, $c_3 = -0.005$, $c_5 = 0.003$, and $c_6 = -0.008$.[2] From these numbers it follows that nonleptonic weak decays are driven by the terms proportional to the operators Q_+ and Q_-, while all other terms can be neglected.

It is straightforward to verify that the operator Q_- triggers decays with $\Delta I = 1/2$, while the operator Q_+ induces transitions both in the $\Delta I = 1/2$ and in the $\Delta I = 3/2$ channel. Hence, in order to explain the $\Delta I = 1/2$ rule, one needs to understand the dynamical mechanism which enhances the contribution of the term proportional to Q_-.

Accounting only for weak interactions, one finds $c_+ = c_- = 1$ and $c_3 = c_5 = c_6 = 0$. Clearly, perturbative strong forces do indeed provide a relatively small enhancement of $\Delta I = 1/2$ transitions. On the other hand, a factor of 10 is still missing in order to reproduce the experimental data. This must necessarily come from the nonperturbative sector of QCD. In the OPE formalism, large-distance strong dynamics enters through the low-energy matrix elements of the effective Hamiltonian (1). Hence, we conclude that nonleptonic weak decays are driven by nonperturbative forces which enhance by roughly 1 order of magnitude the hadronic matrix elements of Q_-, relative to the matrix elements of Q_+.

Significant progress in trying to understand these nonperturbative effects has been made in a series of works by Stech, Neubert, Xu, and Dosch (SNXD) [17,23–26]. Their starting point was the observation that the effective Hamiltonian could be Fierz transformed into

$$
\begin{aligned}
H_{\text{eff}} = \frac{G_F}{\sqrt{2}} V_{ud}V_{us}\{&c_-(\mu)(ud)^\dagger_{3^*}(su)_{3^*} + c_+(\mu)(ud)^\dagger_6(su)_6 \\
&+ \cdots + \text{H.c.}\},
\end{aligned} \tag{3}
$$

where $(su)_{3^*} = e_{ikj}s_i^T C(1-\gamma_5)u_j$ is a scalar and pseudoscalar color antitriplet diquark current, while $(su)_6$ is the corresponding color sextet current (the other currents are given by similar expressions). From (3) it follows immediately that the matrix elements proportional to $c_-(\mu)$ will be greatly enhanced if the nonperturbative quark-quark interaction is very attractive in the color antitriplet channel. This is most evident in hyperons: If the nonperturbative forces are so strong to allow, say, a s and u valence quarks in a Σ^+, to form a 0^+ antitriplet quasibound state, then these quarks will have a much larger chance to be caught in the same point and annihilated by the local $(su)_{3^*}$ operator in the effective Hamiltonian. A similar argument can be formulated also in the case of kaon decays.[3] Based on this simple dynamical assumption, SNXD proposed a phenomenological model which simultaneously explains kaon and hyperon nonleptonic decays.

In order to justify the phenomenological assumptions of the SNXD model and make contact with QCD, we need to identify some nonperturbative gauge configurations which, on the one hand, play an important role in the hadron internal dynamics and, on the other hand, generate color antitriplet quasibound diquarks. Instantons have precisely this property. In [13] it was shown that the 't Hooft interaction does indeed form a bound antitriplet *scalar* diquark of mass of roughly 400 MeV. It is therefore natural to ask whether these fields can provide the microscopic mechanism underlying the $\Delta I = 1/2$ rule.

III. LOW-ENERGY MATRIX ELEMENTS

Nonleptonic hyperon decays can be parametrized in terms of two constants corresponding to parity-violating and parity-conserving transitions:

$$
\langle B'\pi|H_{\text{eff}}|B\rangle = i\bar{u}_{B'}[A - B\gamma_5]u_B, \tag{4}
$$

where B (B') denotes the initial (final) baryon, and A and B are, respectively, called *S-wave* and *P-wave* amplitudes. The calculation of these amplitudes is generally performed by analyzing separately two different contributions which correspond to different mechanisms through which the pion in the final state in (4) can be produced.

In the so-called "factorization" part of the amplitude [27], the final meson is excited directly by the color singlet axial-vector current present in the effective Hamiltonian (as pictured in Fig. 1). The corresponding parity-conserving and parity-violating amplitudes for nonleptonic hyperon decays with π^- in the final-state are [17]

$$
\begin{aligned}
A_{ji}^{\pi^-(\text{fact})} &= \left[c_1(\mu) + 2c_6(\mu)\frac{v v'}{m_K^2}\right]F_\pi(M_i - M_j)F_{j,i}^{4+i5}, \\
B_{ji}^{\pi^-(\text{fact})} &= -\left[c_1(\mu) - 2c_6(\mu)\frac{v^2}{m_K^2}\right]F_\pi(M_i + M_j)G_{j,i}^{4+i5} \\
&\quad \times\left(1 + \frac{m_\pi^2}{m_K^2 - m_\pi^2}\right),
\end{aligned} \tag{5}
$$

with

[2] For an explicit expression of the Wilson coefficients see [22].

[3] In this case the diquark is formed out of a valence and a sea quark.

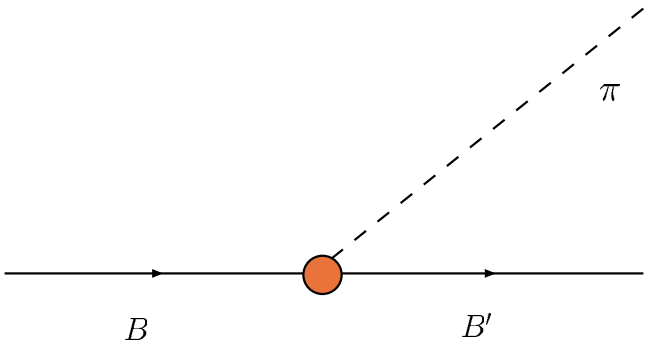

FIG. 1 (color online). Factorization contribution to the nonleptonic hyperon decay $\langle \pi B' | H_{\rm eff} | B \rangle$.

$$\upsilon = \frac{m_\pi^2}{m_u + m_d} \approx \frac{m_K^2}{m_s + m_u}, \qquad \upsilon' = \frac{m_K^2}{m_s - m_u}, \qquad F_\pi = 132 \text{ MeV}. \tag{6}$$

Decay amplitudes with π^0 in the final state are obtained from the substitution

$$\begin{aligned} A_{ji}^{\pi^0(\text{fact})} &= -\frac{1}{\sqrt{2}} A_{\pi^-}^{\text{fact}}(c_1 \to -c_2, F^{4+i5} \to F^{6+i7}), \\ B_{ji}^{\pi^0(\text{fact})} &= -\frac{1}{\sqrt{2}} B_{\pi^-}^{\text{fact}}(c_1 \to -c_2, F^{4+i5} \to F^{6+i7}). \end{aligned} \tag{7}$$

In (5) the i and j indices select the baryons in the initial and the final state, and the constants F_{ji} and G_{ji} are the axial-vector and vector form factors at zero momentum transfer, defined as

$$\begin{aligned} \langle B_j(1/2^+) | J_\mu^a | B_i(1/2^+) \rangle_{k_\mu \to 0} &= F_{ji}^a \bar{u}(j) \gamma_\mu u(i), \\ \langle B_j(1/2^+) | J_{5\mu}^a | B_i(1/2^+) \rangle_{k_\mu \to 0} &= G_{ji}^a \bar{u}(j) \gamma_\mu \gamma_5 u(i). \end{aligned} \tag{8}$$

Assuming $\mathrm{SU}_f(3)$ flavor symmetry and using the Goldberger-Treiman relation we have

$$\begin{aligned} g_{ji}^a &= \sqrt{2}(i f_{jai} F + d_{jai} D) g \\ \text{with } g_{ji}^a &= \frac{\sqrt{2}}{F_\pi} G_{ji}^a (M_j + M_i), \qquad F_{ji}^a = i f_{jai}. \end{aligned} \tag{9}$$

Notice that, in the flavor symmetric limit, the factorization part of the amplitudes is completely determined in terms of experimentally measured low-energy constants. In this work, we use the values [24]

$$g = 13.5, \qquad F + D = 1, \qquad \frac{D}{F} \simeq 1.8, \tag{10}$$

where the D/F ratio is extracted from semileptonic decays [28].

It is immediate to verify that factorization amplitudes alone cannot explain the nonleptonic low-energy decays of kaons and hyperons.[4]

[4]On the other hand, factorization gives the dominant contribution in energetic B and D nonleptonic decays [27].

The leading contribution to such reactions emerges from a soft-pion analysis of the matrix element (4). By applying the PCAC relation, the pion in the final state is replaced by an additional operator, expressing the divergence of the axial-vector current:

$$\begin{aligned} \langle B_j \pi^a(q) | H_{\rm eff}(0) | B_i \rangle = \lim_{q^2 \to m_\pi^2} i \frac{\sqrt{2}(-q^2 + m_\pi^2)}{F_\pi m_\pi^2} \\ \times \int d^4x \, e^{iqx} \langle B_j | T[\partial^\mu J_{5\mu}^a(x) \\ \times H_{\rm eff}(0)] | B_i \rangle. \end{aligned} \tag{11}$$

One then applies the well-known identity

$$\begin{aligned} i \int d^4x \, T[\partial^\mu J_{5\mu}^a(x) H_{\rm eff}(0)] e^{iqx} \\ = q^\mu \int d^4x \, T[J_{5\mu}^a(x) H_{\rm eff}(0)] - i[I_5^a, H_{\rm eff}] \end{aligned} \tag{12}$$

(I_5^a is the axial-charge operator) and performs the analytic continuation to $q_\mu \to 0$ (soft-pion hypothesis).

The first term on the right-hand side of (12) leads to the so-called "pole contribution." Physically, it corresponds to the processes in which the effective Hamiltonian mixes the initial or final baryon with some intermediate virtual state (see Fig. 2). The final results for the pole contributions read

$$\begin{aligned} B_{ji}^{(\text{pole})} &= \frac{\sqrt{2}(M_j + M_i)}{F_\pi} \left[\frac{G_{jl} h_{li}^+}{(M_i - M_l)} + \frac{h_{jl}^+ G_{li}}{(M_j - M_l)} \right] A_{ji}^{(\text{pole})} \\ &= -\frac{\sqrt{2}}{F_\pi} [E_{jl} h_{li}^- - h_{jl}^- E_{li}], \end{aligned} \tag{13}$$

where M^* denotes the masses of the intermediate $B_l(1/2^-)$ baryon which is mixed with the $1/2^+$ baryon by the effective Hamiltonian. The low-energy constants

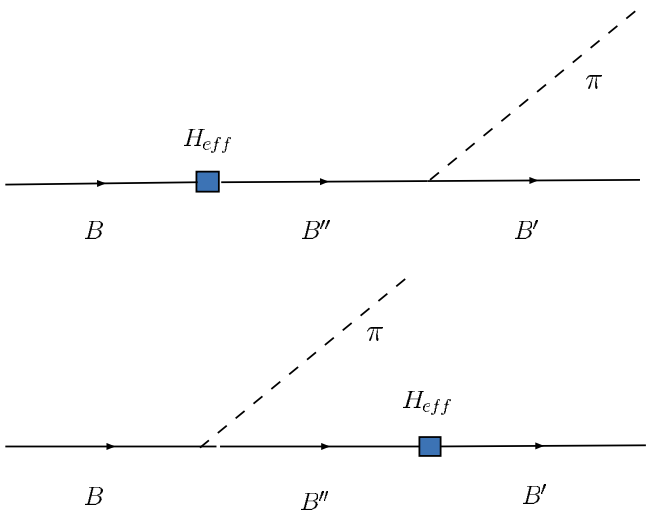

FIG. 2 (color online). Pole contributions to the nonleptonic hyperon decay $\langle \pi B' | H_{\rm eff} | B \rangle$.

$h_{ji}^{+(-)}$ and E_{ji}^{a} are defined as

$$\begin{aligned}\langle B_j(1/2^+)|H_{\rm eff}^{pc}|B_i(1/2^+)\rangle &= h_{ji}^{+}\bar{u}(j)u(i),\\ \langle B_j(1/2^+)|H_{\rm eff}^{pv}|B_i(1/2^-)\rangle &= h_{ji}^{-}\bar{u}(j)u(i),\\ \langle B_j(1/2^-)|J_{5\mu}^{a}|B_i(1/2^+)\rangle_{k_\mu\to 0} &= E_{ji}^{a}\bar{u}(j)\gamma_\mu u(i).\end{aligned} \tag{14}$$

$H_{\rm eff}^{pc}$ is the parity-conserving part of the effective Hamiltonian, and reads

$$\begin{aligned}H_{\rm eff}^{pc} = \tilde{A}[&\epsilon_{ijk}(\bar{d}_i C\bar{u}_j)\epsilon_{lmk}(d_l C\bar{u}_m)\\ &+ \epsilon_{ijk}(\bar{d}_i C\gamma_5\bar{u}_j)\epsilon_{lmk}(d_l C\gamma_5\bar{u}_m)],\end{aligned} \tag{15}$$

where

$$\tilde{A} = \frac{G_F}{\sqrt{2}}\sin\theta_c\cos\theta_c c_-(\mu). \tag{16}$$

$H_{\rm eff}^{pv}$ is the parity-violating part of the effective Hamiltonian and reads

$$\begin{aligned}H_{\rm eff}^{pv} = -\tilde{A}[&\epsilon_{ijk}(\bar{d}_i C\bar{u}_j)\epsilon_{lmk}(d_l C\gamma_5\bar{u}_m)\\ &+ \epsilon_{ijk}(\bar{d}_i C\gamma_5\bar{u}_j)\epsilon_{lmk}(d_l C\bar{u}_m)].\end{aligned} \tag{17}$$

Using $SU_f(3)$ symmetry, one can express these matrix elements in terms of few coefficients:

$$\begin{aligned}h_{ji}^{\pm} &= 2\sqrt{2}(if_{j6i}f^{\pm} + d_{j6i}d^{\pm}), \qquad h_{j0}^{-} = e\delta_{j6},\\ E_{ji}^{a} &= 2\sqrt{2}(if_{jai}F^{-} + d_{jai}D^{-}), \qquad E_{0i}^{a} = E\delta_{ia}.\end{aligned} \tag{18}$$

In addition to the pole part, the S-wave amplitudes receive also a contribution coming from the commutator in (12).[5] This is usually referred to as the "soft-pion" term:

$$A_{ji}^{a(\rm soft)} = \frac{-\sqrt{2}}{F_\pi}\langle B_j|[I_5^a, H_{\rm eff}]|B_i\rangle. \tag{19}$$

Unlike the factorization part, the pole and soft-pion terms involve matrix elements which are not directly related to experiments and have to be estimated theoretically. In the next section we present our calculation of these matrix elements in the ILM.

IV. ILM CALCULATION

In this section we present our calculation of the P-wave and S-wave amplitudes, within the ILM.

A. P-wave amplitudes

In order to determine the P-wave amplitudes in the ILM model, we need to evaluate the nonperturbative inputs h_{ji}^{+}, defined in (14).

In a field-theoretic framework, these matrix elements can be extracted from appropriate ratios of Euclidean three- and two-point functions. Let us consider the three-point correlator:

$$\begin{aligned}G_3^{B'B}(\tau) = &\int d^3\mathbf{x}\int d^3\mathbf{y}\\ &\times\langle 0|T[J_{B'}^{\alpha}(\mathbf{x},2\tau)\mathcal{H}_{\rm eff}(\mathbf{y},\tau)\bar{J}_B^{\alpha}(\mathbf{0},0)]|0\rangle,\end{aligned} \tag{20}$$

where $\tau = it$, α is a spinor index, and $J_B^{\alpha}(x)$, $J_{B'}^{\alpha}(x)$ are interpolating operators which excite states with the quantum numbers of the B and B' baryons. [For example, for the proton and Σ^+ hyperon, we used $J_P^{\alpha}(x) = \epsilon_{abc}[u_a^T(x)C\gamma_5 d_b(x)]u_c^{\alpha}(x)$ and $J_{\Sigma^+}^{\alpha}(x) = \epsilon_{abc}[s_a^T(x)C\gamma_5 u_b(x)]u_c^{\alpha}(x)$.]

It is straightforward to show that, in the limit of large Euclidean time separation, the correlator (20) relates directly to the matrix element $h_{B'B}^{+}$:

$$\lim_{\tau\to\infty} G_3^{B'B}(\tau) = 2h_{B'B}^{+}\Lambda'_B\Lambda_B e^{-(M_{B'}+M_B)\tau}, \tag{21}$$

where $\Lambda_{B'}$ and Λ_B are the couplings of the interpolating fields $J_{B'}$ and $J_{B'}$ to the B' and B states, defined as

$$\langle 0|J_B(x)|B\rangle = \Lambda_B u_B(p)e^{ip\cdot x}. \tag{22}$$

In the $SU_f(3)$ symmetric limit we are considering, we have $\Lambda_{B'} = \Lambda_B = \Lambda$ and $M_{B'} = M_B = M$. Hence, in this approximation, it is possible to extract the matrix element $h_{B'B}^{+}$ by taking the ratio of the three-point function (20) with, say, the proton two-point function:

$$h_{B'B}^{+} = \lim_{\tau\to\infty}\frac{G_3^{B'B}(\tau)}{G_2(2\tau)}, \tag{23}$$

where

$$G_2(\tau) = \int d^3\mathbf{x}\langle 0|T[J_P^{\alpha}(\mathbf{x},\tau)\bar{J}_P^{\alpha}(\mathbf{0},0)]|0\rangle \overset{\tau\to\infty}{\to} 2\Lambda^2 e^{-M\tau}. \tag{24}$$

Nonperturbative calculations of QCD correlation functions can be performed by exploiting the analogy between the Euclidean generating functional and the partition function of a statistical ensemble. In lattice QCD, one usually carries out analytically the integral over the fermionic fields, and then computes numerically Monte Carlo averages of the resulting Wick contractions over a statistical ensemble of gauge configurations. In the ILM, we replace the space of all gauge configurations with an ensemble of instantons and anti-instantons [5]. As in lattice QCD, in each configuration the quark propagator is obtained by inverting the Dirac operator. Unlike lattice QCD, in the ILM there is no need of regularization, so all calculations are performed in the continuum. This prescription is equivalent to computing the correlation functions to all orders in the 't Hooft interaction.

In this work we have considered the simplest version of the model, the random instanton liquid (RILM), in which the density and size of the pseudoparticles are kept fixed,

[5] In P-wave amplitudes such a contribution vanishes because the commutator selects only the parity-violating part of the effective Hamiltonian.

TABLE I. Theoretical prediction and experimental results for P-wave amplitudes. Following the standard notation, B_q^Q corresponds to $\mathrm{Amp}(B^Q \to B' + \pi^q)$. The RILM prediction is obtained by adding the pole and factorization contribution. Wilson coefficients have been evaluated at the hadronic scale $\mu = 1/\bar{\rho} = 0.6$ GeV, using $\Lambda_{\overline{MS}} = 230$ MeV.

		Pole	Factorization	RILM	Experiment	$\frac{\text{RILM}}{\text{Exp.}}$
P-wave amplitudes ($\times 10^7$)	Λ_0^0	-6.87	-4.03	-10.9 ± 1.17	-15.61 ± 1.4	0.7
	Λ_-^0	9.72	8	17.71 ± 1.66	22.40 ± 0.54	0.8
	Σ_0^+	20.82	1.65	22.4 ± 3.55	26.74 ± 1.32	0.8
	Σ_+^+	31.84	0	31.84 ± 4.81	41.83 ± 0.17	0.8
	Σ_-^-	1.75	-3.26	-1.52 ± 0.30	-1.44 ± 0.17	1.1
	Ξ_-^-	16.15	-2	14.15 ± 2.75	17.45 ± 0.58	0.8
	Ξ_0^0	-11.42	1.01	-10.42 ± 1.95	-12.13 ± 0.71	0.9

while their position in a periodic box and their color orientation are generated according to a random distribution.

We have evaluated numerically [29] the correlation functions associated to the matrix elements $\langle p|H_{\mathrm{eff}}|\Sigma^+\rangle$ and $\langle\Lambda|H_{\mathrm{eff}}|\Xi^0\rangle$. We have averaged over 52 configurations of 252 pseudoparticles of size $\rho = 0.33$ fm, in a periodic box of volume $(3.6^3 \times 5.4)$ fm^4. As in lattice simulations, we have chosen a rather large current quark mass for u and d quarks (75 MeV), to avoid finite-volume artifacts. In order to check for the dependence of our results on the quark masses, we have also performed the same calculation using larger quark masses (135 MeV). Finally, to enforce flavor symmetry, we have set $m_s = m_u = m_d$. The six-dimensional spatial integration in (20) has been performed by means of an adaptive Monte Carlo method (VEGAS). Convergence has been achieved using 1600 integration points. The three-dimensional integral in (24) has been performed by first carrying out the angular integration analytically (exploiting rotational symmetry) and then computing the remaining one-dimensional radial integration by a Gauss-quadrature method.

We have observed that the quark-model relation $f^+/d^+ \simeq 1$ holds also in our field-theoretic approach,[6] with $d^+ = (0.28 \pm 0.05) \times 10^{-7}$ GeV, a result quite close to the prediction of the SNXD model ($d^+ = 0.35 \times 10^{-7}$ GeV [24]). This calculation shows explicitly that gluon and sea degrees of freedom contribute very little to these decay amplitudes.

The results presented thus far correspond to simulations performed with quark masses of 75 MeV. We have found that calculations with heavier quark masses (135 MeV) lead to very similar results ($d^+ = 0.27 \pm 0.04 \times 10^{-7}$ GeV). We can therefore conclude that the dependence of these amplitudes on the quark mass is very weak.

[6]We remark that, in a field-theoretic framework, the relation $f^+/d^+ \simeq -1$ is nontrivial. It is a consequence of the fact that the sea contribution from fermionically disconnected graphs is negligible.

It is important to ask whether diquark quasibound states survive within $1/2^+$ baryons, or if they are melted by the interaction with the third quark. To answer, we have compared matrix elements obtained from the scalar and from the pseudoscalar part of the diquark operator in (3). We have found that such matrix elements are indeed dominated by the *scalar* operators in the effective Hamiltonian. This is a nontrivial result which represents clean signature of the existence of *scalar* diquark structures in the hyperons, in the ILM. On the other hand, it also implies that pseudoscalar diquarks are not present in such baryons. Finally, since final-state interaction effects are presumably small in this channel [24], we have neglected them.

Our results for the P-wave amplitudes, obtained by collecting the factorization and the pole contributions, are reported in Table I and compared to experimental data. First of all, we observe that the RILM can reproduce the overall body of data on P-wave hyperon decays. All theoretical amplitudes lie within approximately 20% from the experimental results. Note that this discrepancy is of the order of the systematic error introduced by the assumption of $\mathrm{SU}_f(3)$ symmetry. However, taking a closer look, we notice that the central values of the theoretical predictions consistently undershoot the experimental results (except in one case to be discussed below). This is hardly surprising, because in the present calculation we have neglected all confining interactions.

Finally, we observe that the theoretical prediction for the amplitude Σ_-^- is the only one overshooting the experimental data. This is probably a reflection of the fact that this is a very delicate channel, where the factorization and pole terms are of the same order of magnitude and have opposite sign.

B. *S*-wave amplitudes

S-wave amplitudes, receive contributions from both the pole and the soft-pion part of the PCAC amplitudes.

The pole part involves mixing of $1/2^+$ baryons with $1/2^-$ virtual intermediate states (14). In the simple quark-diquark model discussed in [17], 0^- diquarks in

TABLE II. Theoretical prediction and experimental results for S-wave amplitudes. Following the standard notation, A_q^Q corresponds to Amp($B^Q \to B' + \pi^q$). The RILM prediction is obtained by adding the soft-pion and factorization contributions. The results in RILM(FSI) include also final-state interaction corrections, as estimated in [24]. Wilson coefficients have been evaluated at the hadronic scale $\mu = 1/\bar{\rho} = 0.6$ GeV, using $\Lambda_{\overline{MS}} = 230$ MeV.

		Soft	Factorization	RILM	RILM(FSI)	Experiment	$\frac{\text{RILM}}{\text{Exp.}}$
S-wave amplitudes ($\times 10^7$)	Λ_0^0	-1.71	0.2	-1.51	-1.75 ± 0.34	-2.36 ± 0.03	0.7
	Λ_-^0	2.41	-0.53	1.88	2.25 ± 0.57	3.25 ± 0.02	0.7
	Σ_0^+	-4.18	0.23	-3.96	-3.55 ± 0.64	-3.25 ± 0.02	1.1
	Σ_+^+	0	0	0	0	0.14 ± 0.03	$\cdots$
	Σ_-^-	5.91	-0.62	5.29	4.34 ± 0.9	4.27 ± 0.01	1
	Ξ_-^-	-4.83	0.61	-4.22	-4.22 ± 0.82	-4.49 ± 0.02	0.9
	Ξ_0^0	3.41	-0.22	3.20	3.20 ± 0.58	3.43 ± 0.06	0.9

octet $1/2^-$ baryons were introduced to obtain nonvanishing h_{ij}^- matrix elements. On the other hand, the 't Hooft interaction is repulsive in the 0^- channel. While the attraction in the 0^+ channel triggers the formation of scalar diquarks in $1/2^+$ hyperons contributing to P-wave amplitudes, the repulsion in the 0^- channel prevents the formation of pseudoscalar diquarks, which would show up in $1/2^-$ hyperons. Hence, in the ILM, the pole contribution to S-wave amplitudes is expected to be suppressed and we shall neglect it.

On the other hand, we compute explicitly the soft-pion term (19), which arises from the commutator in (12). For the sake of definiteness, let us consider the $\langle P\pi^0|H_{\text{eff}}|\Sigma^+\rangle$ S-wave transition. The relevant part of the Q_- operator in the effective Hamiltonian can be written in a simplified notation as

$$(du)^\dagger_{0^+}(us)_{0^-} + (du)^\dagger_{0^-}(us)_{0^+} + \text{H.c.} \tag{25}$$

The soft-pion contribution depends on the commutator of the effective Hamiltonian with the axial-charge operator. Using current-algebra relationships, it is possible to show that the commutator of (25) with I_5^a gives the same result as the commutator of the operator:

$$(du)^\dagger_{0^+}(us)_{0^+} + (du)^\dagger_{0^-}(us)_{0^-} + \text{H.c.}, \tag{26}$$

with the I^a operator. Because of the repulsion of the 't Hooft interaction in the 0^- diquark channel, the instanton contribution to the matrix elements of the second term in (26) between $1/2^+$ states is negligible. On the other hand, the matrix elements of the first term in (26) relate to the f^+ and d^+ constants, which have been calculated to determine the P-wave amplitudes.

Final-state interaction corrections in this channel are rather small but not negligible. We have included them following the estimate performed in [23].

The RILM predictions for S-wave decay amplitudes are presented in Table II and compared to experimental results. As in the case of P-wave transitions, we observe a good agreement with experiment, with prediction within 20% from the data. Again, we observe that the ILM tends to undershoot the measured amplitudes, which confirms the idea that roughly 20% of the attraction in the 0^+ antitriplet channel comes from confining interactions. Note that having neglected pole terms leads to very reasonable results (except in one channel, Σ_+^+, where also all other contributions vanish). Clearly, there is no need to assume pseudoscalar diquark structures in $1/2^-$ baryons.

V. DISCUSSION

In the previous section we have shown that the inclusion of instanton-induced effects allows one to reproduce the overall body of data on nonleptonic hyperon decays. We recall that both P-wave and S-wave results have been obtained by considering only the contribution of the operator Q_- in the effective Hamiltonian, which drives only transitions with violation of isospin 1/2. Hence, we conclude that the 't Hooft interaction does provide a nonperturbative dynamical explanation of the $\Delta I = 1/2$ rule.

An important question to ask is whether one can rule out alternative dynamical mechanisms, which are not based on quasiclassical interactions. As already stressed, the essential dynamical property which is required in order to produce an enhancement of $\Delta I = 1/2$ transitions is an attraction in the scalar antitriplet 0^+ channel. Clearly, any model for the microscopic dynamics which exhibits a sufficiently strong attraction in this channel will produce scalar diquarks.[7] It is nevertheless very important to clarify the dynamical origin of these structures, whose existence seems to be confirmed by a number

[7]For example, also a model built on the extension of the one-gluon-exchange interaction into the nonperturbative regime will do the job, at least on a qualitative level. For a recent quark-model calculation, based on a nonrelativistic spin-dependent potential, see [30].

of independent phenomenological studies (for example, in connection with exotic spectroscopy, see [31,32]).

In the following we suggest a systematic, model-independent procedure to answer the question whether quasiclassical topological fields do indeed provide the dominant nonperturbative interactions driving diquark formation and the $\Delta I = 1/2$ rule. The idea is to evaluate the relevant matrix elements on the lattice and to compare the behavior under cooling of the decay amplitudes and of the string tension.

The cooling algorithm consists of performing statistical averages on different ensembles of gauge configurations which are closer and closer to the extreme of the Euclidean action. This way, the contribution of quasiclassical fields is progressively isolated. It is well known that, after few cooling steps, all perturbative fluctuations as well as the confining interactions are removed from the QCD vacuum. On the other hand, the essential properties of light hadrons, such as their masses and point-to-point correlators, are seen to change very little. This implies that light hadrons are predominantly bound by quasiclassical nonconfining gauge configurations [6].

The main shortcoming of the cooling procedure is that it leads to results which intrinsically depend on the arbitrary number of cooling steps. Because of this problem, it is very difficult to make systematic, *quantitative* statements. On the other hand, the *qualitative* observation that light hadrons still exist in the absence of confinement and that smooth, topological structures survive even when the string tension is drastically suppressed are model-independent facts, in QCD.

We recall that instantons are smooth, topological quasiclassical configurations which bind hadrons but do not confine. This observation suggests to study the behavior of the $\Delta I = 1/2$ decay amplitudes as a function of the string tension, calculated after each cooling step (see Fig. 3). On the basis of our analysis we predict that, if instantons are indeed the leading dynamical effect, then the amplitudes should decrease by at most 20%, as the string tension varies from its physical value to nearly zero. On the other hand, if instantons do not provide the dominant interaction in these processes, then the amplitudes should drastically die out, along with the string tension.

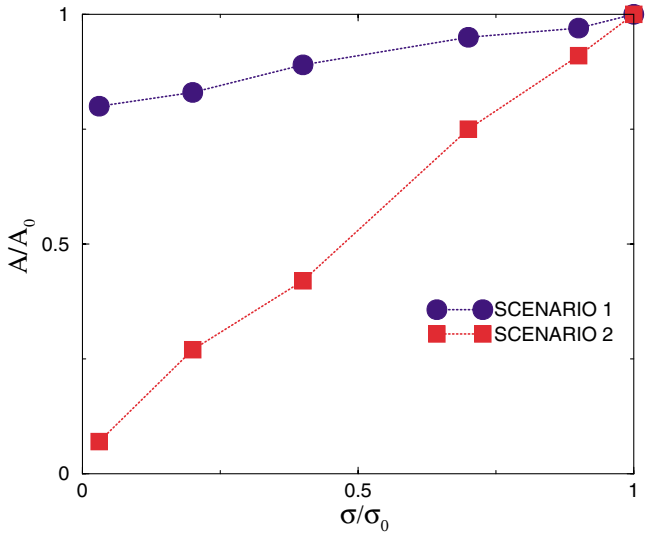

FIG. 3 (color online). Two different hypothetical scenarios for the behavior of lattice QCD decay amplitudes under cooling. On the x axis, σ/σ_0 represents the values for string tension obtained after different numbers of cooling steps, normalized to the QCD string tension (no cooling). On the y axis, A/A_0 represents the ratio of a decay amplitude computed after the same number of cooling steps, normalized to its value in QCD (no cooling). In scenario 1, the decays are driven by quasiclassical interactions and the amplitudes change by roughly 20% under cooling (ILM prediction). In scenario 2, the decays are driven by the confining forces and vanish rapidly under cooling.

VI. CONCLUSIONS AND OUTLOOK

In this work, we have studied the instanton contribution to nonleptonic weak decays of hyperons. We have applied the OPE formalism to separate hard-gluon corrections to soft nonperturbative effects and we have used the random instanton liquid model to compute the relevant low-energy matrix elements. The connection between the matrix elements and the decay amplitudes has been established considering the contributions arising from both the pole and soft-pion terms in the PCAC relations and from the factorization part of the amplitude. Final-state interaction corrections have been applied to S-wave transitions, and have been neglected in P-wave transitions.

We have found that the ILM yields to a good description of both P-wave and S-wave decays, providing a microscopic explanation for the $\Delta I = 1/2$ rule. In this model, the strong enhancement of the transitions in which the total isospin is changed by $1/2$ units is originated by the strong attraction due to the 't Hooft interaction in the quark-quark scalar antitriplet channel, leading to a quark-diquark structure in the hyperons. We stress that the calculations presented in this work were performed with no parameter fitting. The only phenomenological quantities introduced by the ILM are the instanton average size and density, which had been fixed long ago to reproduce global vacuum properties.

Our results provide a further confirmation of the generally accepted picture according to which the internal dynamics of light hadrons is dominated by the interactions responsible for chiral symmetry breaking. Indeed in the present calculation, roughly 70% of the amplitudes comes from instanton-induced interactions (which drive the spontaneous breaking of chiral symmetry), 10% from hard-gluon-exchange corrections, while the remaining 20% is due to some other interactions, presumably related

to confinement. Results are seen to depend very weakly on the value of the current quark masses chosen.

Since the present analysis is affected by some model dependence, we cannot in principle rule out possible alternative dynamical mechanisms for scalar diquark formation. However, we have suggested a lattice-based procedure which would allow one to determine, in an unambiguous and model-independent way, if the strong attraction in the diquark channel is generated by quasiclassical gauge configurations or if it is due to the quantum fluctuations associated with the dynamics of color confinement.

ACKNOWLEDGMENTS

We thank D. Jido and V. Vento for very useful conversations. P. F. acknowledges interesting discussions with J.W. Negele and R. L. Jaffe. Feynmann diagrams have been drawn using JaxoDraw [33].

[1] J. F. Donoghue, E. Golowich, and B. R. Holstein, *Dynamics of the Standard Model* (Cambridge University Press, Cambridge, England, 1992).
[2] J. G. Koerner, Nucl. Phys. **32**, 282 (1970); J. C. Pati and C. H. Woo, Phys. Rev. D **3**, 2920 (1971).
[3] J. F. Donoghue, E. Golowhich, and B. Holstein, Phys. Rep. **131**, 319 (1986).
[4] G. 't Hooft, Phys. Rev. Lett. **37**, 8 (1976); Phys. Rev. D **14**, 3432 (1976).
[5] T. Schäfer and E.V. Shuryak, Rev. Mod. Phys. **70**, 323 (1998).
[6] M. C. Chu, J. M. Grandy, S. Huang, and J.W. Negele, Phys. Rev. D **49**, 6039 (1994).
[7] T. A. DeGrand and A. Hasenfratz, Phys. Rev. D **64**, 034512 (2001).
[8] P. Faccioli and T. A. DeGrand, Phys. Rev. Lett. **91**, 182001 (2003).
[9] P. Boucaud *et al.*, J. High Energy Phys. 04 (2003) 005
[10] D. Diakonov, in Proceedings of the "Enrico Fermi" School in Physics, Varenna, 1995 (hep-ph/9602375).
[11] E.V. Shuryak, Nucl. Phys. B **214**, 237 (1982).
[12] E.V. Shuryak and J. J. M. Verbaarschot, Nucl. Phys. B **140**, 37 (1993).
[13] T. Schaefer, E.V. Shuryak, and J. J. M. Verbaarschot, Nucl. Phys. B **412** 143 (1994).
[14] P. Faccioli, Phys. Rev. D **65**, 094014 (2002).
[15] P. Faccioli, hep-ph/0312019.
[16] P. Faccioli, A. Schwenk, and E.V. Shuryak, Phys. Rev. D **67**, 113009 (2003).
[17] B. Stech, Phys. Rev. D **36**, 975 (1987).
[18] N. I. Kochelev and V. Vento, Phys. Rev. Lett. **87**, 111601 (2001).
[19] D. Horvat, Z. Narancic, and D. Tadic, Phys. Rev. D **51**, 6277 (1995).
[20] P. Faccioli and E.V. Shuryak, Phys. Rev. D **64**, 114020 (2001).
[21] M. A. Shifman, A. I. Vainshtein, and V. I. Zakharov, Sov. Phys. JETP **45**, 670 (1977) [Zh. Eksp. Teor. Fiz. **72**, 1275 (1977)]; F. J. Gilman and M. B. Wise, Phys. Rev. D**20**, 2392 (1979).
[22] G. Buchalla, A. Buras, and M. Harlander, Nucl. Phys. B **337**, 313 (1990).
[23] B. Stech and Q. P. Xu, Z. Phys. C **49**, 491 (1991).
[24] H. D. Dosch, M. Jamin, and B. Stech, Z. Phys. C **42**, 167 (1989).
[25] M. Neubert, Z. Phys. C **50**, 243 (1991).
[26] M. Neubert and B. Stech, Phys. Rev. D **44**, 775 (1991).
[27] B. Stech, Nucl. Phys. B (Proc. Suppl.) 1, 17 (1988), and references therein.
[28] D. F. Donoughue, B. R. Holstein, and S.W. Klimt, Phys. Rev. D **35**, 2903 (1987).
[29] For details, see M. Cristoforetti, Tesi di Laurea, Università di Milano, 2004.
[30] E. Hiyama *et al.*, Phys. Rev. D **69**, 094012 (2004).
[31] R. L. Jaffe and F. Wilczek, Phys. Rev. Lett. **91**, 232003 (2003).
[32] E.V. Shuryak and I. Zahed, Phys. Lett. B **589**, 21 (2004).
[33] D. Binosi and L. Theussl, Comput. Phys. Commun. **161**, 76 (2004).